# DETECTION OF HOUSING AND AGRICULTURE AREAS ON DRY-RIVERBEDS FOR THE EVALUATION OF RISK BY LANDSLIDES USING LOW-RESOLUTION SATELLITE IMAGERY BASED ON DEEP LEARNING. STUDY ZONE: LIMA, PERU

**Anonymous authors**
Paper under double-blind review

## ABSTRACT

The expansion of human settlements in Peru has caused risk exposure to landslides. However, this risk could increase because the intensity of the El niño phenomenon will be greater in the coming years, increasing rainfall on the Peruvian coast. In this paper, we present a novel methodology for detecting housing areas and agricultural lands in low-resolution satellite imagery in order to analyze potential risk in case of unexpected landslides. It was developed by creating two datasets from Lima Metropolitana in Peru, one of which is for detecting dry riverbeds and agriculture lands, and the other for classifying housing areas. We applied data augmentation based on geometrical methods and trained architectures based on U-net methods separately and then, overlap the results for risk assessment. We found that there are areas with significant potential risk that have been classified by the Peruvian government as medium or low risk areas. On this basis, it is recommended obtain a dataset with better resolution that can identify how many housing areas will be affected and take the appropriate prevention measures. Further research in post-processing is needed for suppress noise in our results.

## 1 INTRODUCTION

The detection of landslides in satellite images has received great attention in recent years, due to its relationship with urban planning and land use. Based on the research of Wang et al [1], El Niño phenomenon will have greater intensity in the coming years, whose effects will generate landslides and floods in the South American Pacific coastal area, but it is in Peru where the effects of this phenomenon have a greater socioeconomic impact due to its geographical location, poor urban planning and the activation of dry riverbeds [1] that had remained passive for years, as observed in 2017, when there was at least three hundred and seventy two thousand damaged homes, according to statistics from INDECI [2].

One of the ways to analyze this problem is to have information about the landslide susceptibility which it has received extensive research. Moayedi et al.[3] developed a hybrid model called PSO-ANN to create landslide susceptibility maps over the city of Kermanshah, Iran, and more recently Ghorbanzadeh et al [4] showed that convolutional neural networks of deep learning have better performance than traditional machine learning methods that use 4-band images from Nepal and China. In addition, there are datasets that contain land cover classification and building footprint detection such as DeepGlove [5], EuroSat [6] and SpaceNet [7] that have promoted the development of different investigations related to semantic segmentation approach [8, 9, 10].

Although there are numerous approaches to the detection of landslides and buildings separately, none analyzes the direct relationship between floods or landslides in populated and agricultural areas. In addition, there is no dataset available focused on Peruvian geography. So this is the main

[1]Dry riverbed is a type of landslide which course is channeled, as shown in Figure 2, and in Peru it is common to find constructions in the course of dry riverbeds as shown in Figure 3

reason a novel approach is developed whose methodology consists in: (1) obtaining two corresponding novel datasets, the first has dry riverbeds, risk areas and agriculture, while the second one has residential, human settlement and industrial areas; (2) the increase of the dataset that performs geometric operations, as well as its preprocessing; (3) The selection of the appropriate deep learning method that can classify pixels; and (4) Fusion of results for risk analysis. Finally, discussion and future work that will be developed for this approach.

## 2 DATASET AND EVALUATION METRIC

The low resolution satellite imagery used for both tasks were collected by RapidEye satellite provided by Planet Labs through its imagery exploration toolkit. This satellite imagery has 3-band natural color (red, green, blue) and a 5m pixel resolution. For the purpose of this research, the full dataset covers a total of 450 $km^2$ of our study zone: Lima, Peru. Each image has been labelled manually using LabelMe software [11] as the selected annotation toolkit. Each image is paired with a ground truth mask[2] , samples are shown in Figure 4 and Figure 5. The masks are images with a total of 3 different classes and depend on the task. Task 1 is for detecting mainly dry riverbeds and agriculture lands and Task 2 for detecting types of housing areas, the descriptions of each class are shown in Table 1 and Table 2.

We carefully annotated our dataset to avoid overlapping in the annotations and they do not always have all of the classes in one image. The annotations are not perfect due to the fact that many areas can be not seen easily to determine for which class belongs.

Table 1: Description of classes for task 1

| Value | Class | RGB | Description |
|---|---|---|---|
| 1 | Dry riverbed | (1,0,0) | channel where used to flow a river |
| 2 | Inhabited land | (0,1,0) | any kind of building |
| 3 | Agriculture land | (1,1,0) | croplands, farms |
| 0 | Background | (0,0,0) | others |

Table 2: Description of classes for task 2

| Value | Class | RGB | Description |
|---|---|---|---|
| 1 | Residential | (0,1,0) | area where housing predominates |
| 2 | Human settlement | (1,0,0) | areas in initial process of colonization |
| 3 | Industrial | (1,1,0) | industrial plant, farm, warehouse |
| 0 | Background | (0,0,0) | others |

We used the mean overlap or dice coefficient(F1 score) as evaluation metric:

$$Dice - Coefficient = \frac{1}{n}\sum_{i=1}^{c=n} S, S = \frac{2TP_c}{2TP_c + FP_c + FN_c}$$

where $TP_c$ stands for true positive pixel in class c applied to the full output of the model in evaluation; $FP_c$, false positive pixels in class c and $FN_c$, false negative pixels in class c. Then the average is computed over all the different classes that we selected depending on the task.

## 3 METHODS

In order to do an evaluation of risk areas, we split the workflow in two tasks, following the flowchart shown in Figure 6. Both tasks are designed like a segmentation-based approach. The first task aims

[2]RGB color code for visualization

to identify mainly dry riverbeds and agriculture lands, and the second task aims to identify different types of housing areas in satellite imagery. The main reason is to overlap the results from both tasks and find the housing areas over dry riverbeds, which implies the housing areas are in potential risk in case of unexpected landslide.

### 3.1 DATA AUGMENTATION

On small-scale dataset, data augmentation has been playing a significant role for deep learning models, since this technique tackles potential problems(i.e. overfitting), improves the distribution of the dataset and the generalization ability of the deep learning model[12]. Since we have a small number of training samples in both tasks, we used data augmentation with different methods which include rescaling, flipping, cropping, rotation and canal shuffling. The data collection for each task described in section 2 has been preprocessed for each semantic segmentation model. For the first task, a large satellite image has been sliced in 100 chips with a size of 590x590 pixels with overlapping, and for the second task the selected size was 512x512 pixels. For both tasks we only considered chips as inputs if they had annotations.

### 3.2 MODEL ARCHITECTURES

Since this is a semantic segmentation approach for multi-class segmentation, three architectures have been implemented and compare each other using the evaluation metric mentioned in section 2. U-Net architecture [13] was initially used for biomedical image segmentation, but it has been proved that it has awesome performance in satellite imagery tasks [14, 15] with small quantities of data. This architecture has two main sequential sides: The first side of the model, known as down-sampling, extracts feature maps by applying 3x3 convolutions using rectified linear unit (ReLU) as activation function, then 2x2 max pooling operation with a stride value of 2. The second side consists in upsampling the feature maps, generated by the downsampling side, then operates with a 2x2 convolution, this will expand it to the original input size. Deep Residual Unet architecture [16] was proposed for road extraction task, this model is based on the combination of the U-Net architecture and residual neural network. The residual unit tackles the degradation problem, so information propagation through the network will not face this issue. Finally, Deep UNet architecture [17], which is also based on U-Net but it uses down-sampling blocks in the downsampling side and up-sampling blocks in the upsampling side. Each model outputs a 2-D matrix, which each pixel is assigned to its corresponding predicted class value.

### 3.3 IMPLEMENTATION DETAILS

The mentioned models were implemented on Tensorflow and have been trained in the cross-entropy loss function. We made comparisons using different optimizers such as SGD, RMS prop, Adam with different learning rate(0.01, 0.001, 0.0005), Nadam and Adadelta. A Nvidia GeForce GTX 1080 was used to train our networks, each of them with 300 epochs and a batch size of 4 images and masks.

## 4 RESULTS

The results of our experiments are based on the validation set. We evaluated the performance of different optimizers mentioned in 3.3 with the architectures and experimental results,based on Figure 1, shows the Adadelta, NAdam and Adam with learning rate of 0.0005 have slightly better performance. Then we computed the evaluation metric of each class, since it is more indicative for the performance of the selected architectures and optimizers.

The results and comparison are shown in Table 3 and Table 4 for each task. The columns shows the best performer architecture with different optimizers and F1 score separated into the classes, then the average with background and without background. For the first task, Unet with Adadelta optimizer generated the best performance and for the second task, Residual Unet with Adadelta optimizer, as well. Samples of the original input image, ground truth and prediction mask from each task are shown Figure 7 and Figure 8.

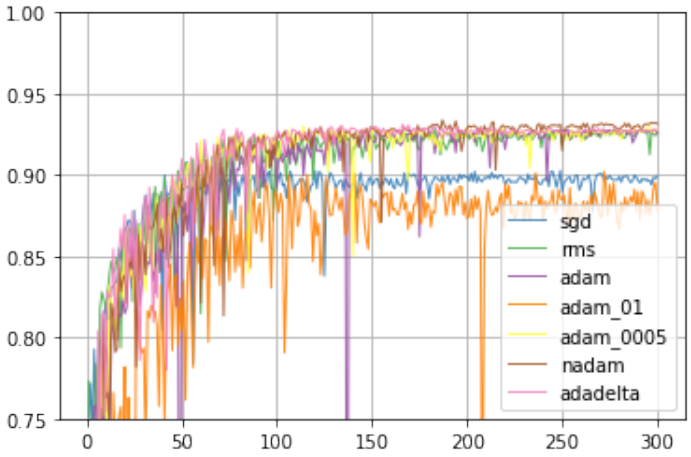


Figure 1: Performance results for the different optimizers.

Table 3: Experimental results for Task 1

| Model | F1 Score | | | | | |
|---|---|---|---|---|---|---|
| | 0 | 1 | 2 | 3 | Avg | Avg (w/o background) |
| Unet + Adam | 0.95 | 0.56 | 0.722 | 0.905 | 0.784 | 0.729 |
| Unet + Adadelta | 0.957 | 0.641 | 0.722 | 0.918 | 0.809 | 0.760 |
| Unet + Adam($l_r$=0.0005) | 0.953 | 0.593 | 0.72 | 0.913 | 0.795 | 0.742 |

Table 4: Experimental results for Task 2

| Model | F1 Score | | | | | |
|---|---|---|---|---|---|---|
| | 0 | 1 | 2 | 3 | Avg | Avg (w/o background) |
| Residual Unet + Adadelta | 0.961 | 0.531 | 0.77 | 0.319 | 0.645 | 0.54 |
| Residual Unet + Adam | 0.963 | 0.551 | 0.803 | 0.232 | 0.637 | 0.529 |
| Residual Unet + NAdam | 0.965 | 0.608 | 0.829 | 0.096 | 0.603 | 0.509 |
| Residual Unet + Adam($l_r$=0.0005) | 0.961 | 0.547 | 0.785 | 0.269 | 0.641 | 0.534 |

## 5 Conclusions and Future Work

In this work, we have proposed a methodology for detecting housing areas in low-resolution satellite imagery in order to analyse potential risk in case of unexpected landslides. The proposed methodology verified that there is housing areas lying on dry riverbeds which implies that these areas are in significant potential risk, even though that these are considered as low susceptibility areas based on the map in Figure 9.

For future work, we will focus on post processing techniques in order to obtained better results, also it is very promising that the performance will improve with different modern semantic segmentation algorithms. It would be beneficial for monitoring the urban planning problem in real time in the Peruvian coast and other places with similar geography.

### Acknowledgments

We thank Planet Labs for providing satellite imagery. The authors were supported by Vice Chancellor for Research from National University of Engineering (VRI-UNI).

## REFERENCES


[1] Bin Wang, Xiao Luo, Young-Min Yang, Weiyi Sun, Mark A Cane, Wenju Cai, Sang-Wook Yeh, and Jian Liu. Historical change of el niño properties sheds light on future changes of extreme el niño. *Proceedings of the National Academy of Sciences*, 116(45):22512–22517, 2019.

[2] MacClune K. Venkateswaran, K. and M.F. Enríquez. El niño costero: The 2017 floods in peru. 2017.

[3] Hossein Moayedi, Mohammad Mehrabi, Mansour Mosallanezhad, Ahmad Safuan A Rashid, and Biswajeet Pradhan. Modification of landslide susceptibility mapping using optimized pso-ann technique. *Engineering with Computers*, 35(3):967–984, 2019.

[4] Omid Ghorbanzadeh, Thomas Blaschke, Khalil Gholamnia, Sansar Raj Meena, Dirk Tiede, and Jagannath Aryal. Evaluation of different machine learning methods and deep-learning convolutional neural networks for landslide detection. *Remote Sensing*, 11(2):196, 2019.

[5] Ilke Demir, Krzysztof Koperski, David Lindenbaum, Guan Pang, Jing Huang, Saikat Basu, Forest Hughes, Devis Tuia, and Ramesh Raska. Deepglobe 2018: A challenge to parse the earth through satellite images. In *2018 IEEE/CVF Conference on Computer Vision and Pattern Recognition Workshops (CVPRW)*, pages 172–17209. IEEE, 2018.

[6] Patrick Helber, Benjamin Bischke, Andreas Dengel, and Damian Borth. Eurosat: A novel dataset and deep learning benchmark for land use and land cover classification. *IEEE Journal of Selected Topics in Applied Earth Observations and Remote Sensing*, 12(7):2217–2226, 2019.

[7] Adam Van Etten, Dave Lindenbaum, and Todd M Bacastow. Spacenet: A remote sensing dataset and challenge series. *arXiv preprint arXiv:1807.01232*, 2018.

[8] Selim S Seferbekov, Vladimir Iglovikov, Alexander Buslaev, and Alexey Shvets. Feature pyramid network for multi-class land segmentation. In *CVPR Workshops*, pages 272–275, 2018.

[9] Chengming Zhang, Yan Chen, Xiaoxia Yang, Shuai Gao, Feng Li, Ailing Kong, Dawei Zu, and Li Sun. Improved remote sensing image classification based on multi-scale feature fusion. *Remote Sensing*, 12(2):213, 2020.

[10] Vladimir Iglovikov, Selim S Seferbekov, Alexander Buslaev, and Alexey Shvets. Ternausnetv2: Fully convolutional network for instance segmentation. In *CVPR Workshops*, volume 233, page 237, 2018.

[11] K. P. Murphy W. T. Freeman B. C. Russell, A. Torralba. Labelme: a database and web-based tool for image annotation. *International Journal of Computer Vision*, 77:157–173,, 2008.

[12] Rui Ma, Pin Tao, and Huiyun Tang. Optimizing data augmentation for semantic segmentation on small-scale dataset. pages 77–81, 06 2019.

[13] Olaf Ronneberger, Philipp Fischer, and Thomas Brox. U-net: Convolutional networks for biomedical image segmentation, 2015.

[14] J. McGlinchy, B. Johnson, B. Muller, M. Joseph, and J. Diaz. Application of unet fully convolutional neural network to impervious surface segmentation in urban environment from high resolution satellite imagery. In *IGARSS 2019 - 2019 IEEE International Geoscience and Remote Sensing Symposium*, pages 3915–3918, July 2019.

[15] D. Hordiiuk, I. Oliinyk, V. Hnatushenko, and K. Maksymov. Semantic segmentation for ships detection from satellite imagery. In *2019 IEEE 39th International Conference on Electronics and Nanotechnology (ELNANO)*, pages 454–457, April 2019.

[16] Zhengxin Zhang, Qingjie Liu, and Yunhong Wang. Road extraction by deep residual u-net. *IEEE Geoscience and Remote Sensing Letters*, 15(5):749–753, May 2018.

[17] Ruirui Li, Wenjie Liu, Lei Yang, Shihao Sun, Wei Hu, Fan Zhang, and Wei Li. Deepunet: A deep fully convolutional network for pixel-level sea-land segmentation, 2017.

# A APPENDIX: SAMPLE OF DRY RIVERBED IN PERU

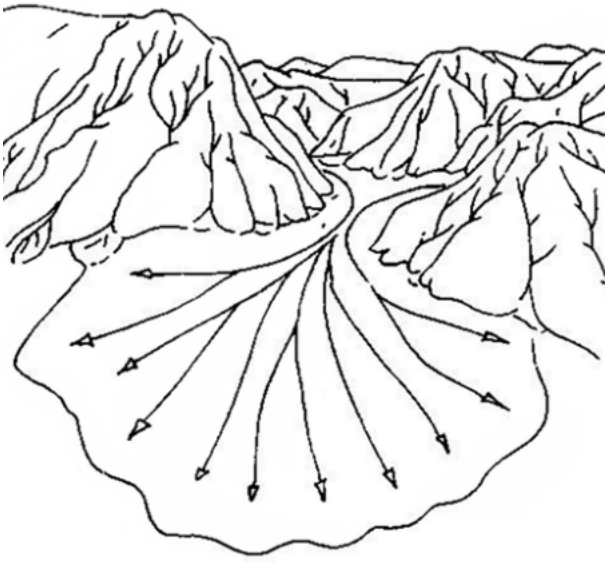

Figure 2: Idealized scheme of the operation of an alluvial fan at the exit of a dry riverbed, with indication of the flow directions. Image from Pedraza, J. Geomorfología: principios, métodos y aplicaciones(Madrid:Rueda, 1996),414


Figure 3: Huaycan - Lima, the yellow lines show the direction of debris flow, the red ones (A) indicate the houses built in the middle of dry riverbed. Image from Villacorta Chambi et al. Peligros geológicos en el área de Lima Metropolitana y la región Callao N°59(Lima:Instituto Geológico, Minero y Metalúrgico,2015)

## B APPENDIX: DATASET VISUALIZATION

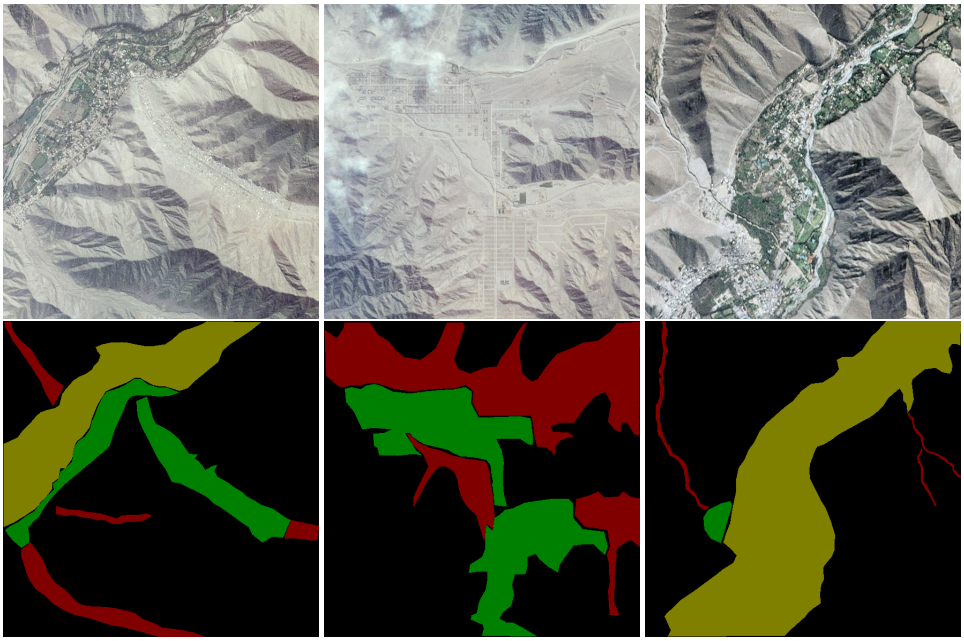

Figure 4: Samples from dataset for Task 1 with the mentioned classes in Table 1

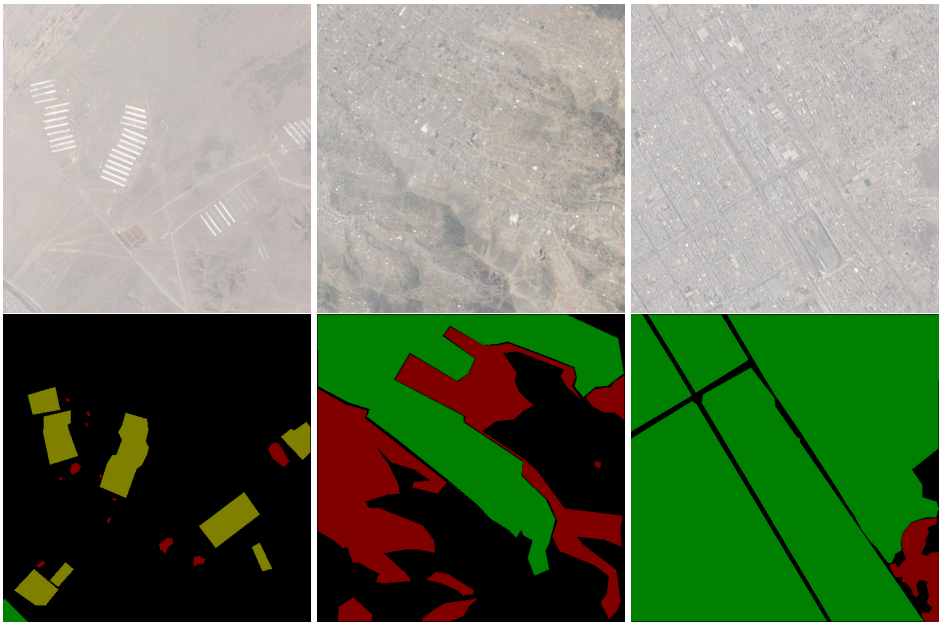

Figure 5: Samples from dataset for Task 2 with the mentioned classes in Table 2

## C APPENDIX: FLOWCHART

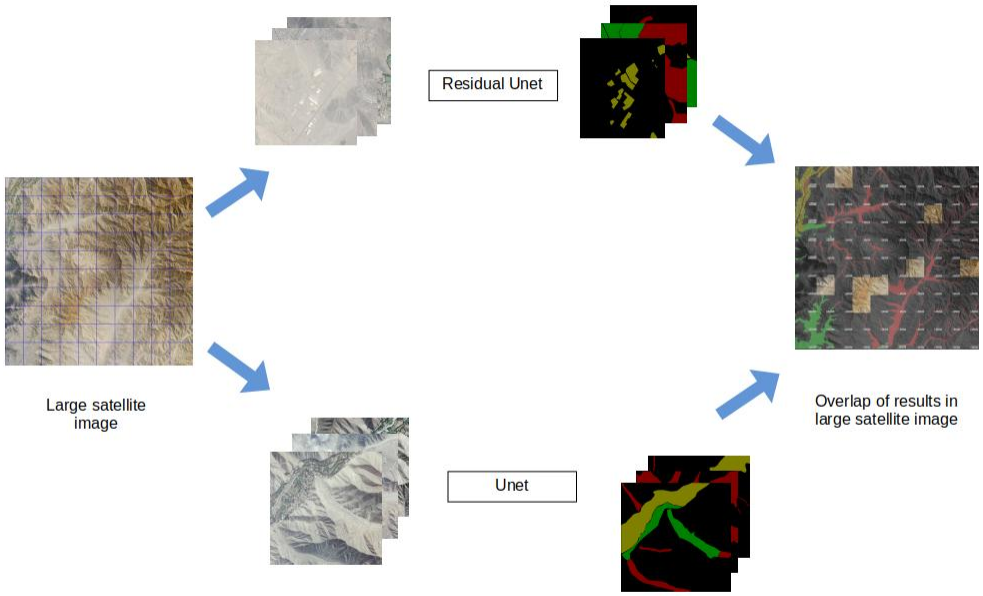


Figure 6: Flowchart of the proposed methodology.

## D APPENDIX: PREDICTIONS

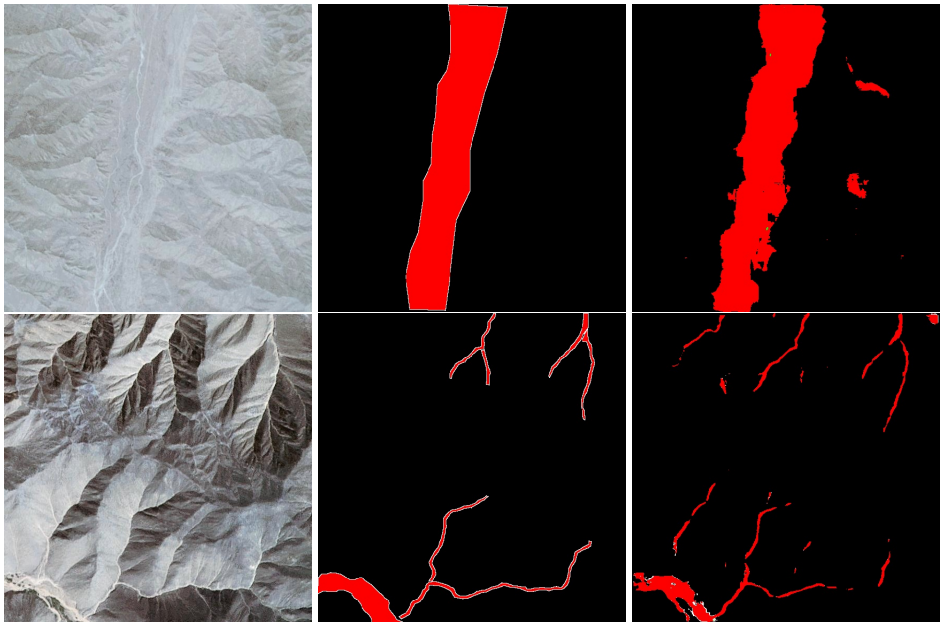

Figure 7: Samples of the results from Task 1. First column has the original images, second column has the ground truth mask an the third has the predicted mask.

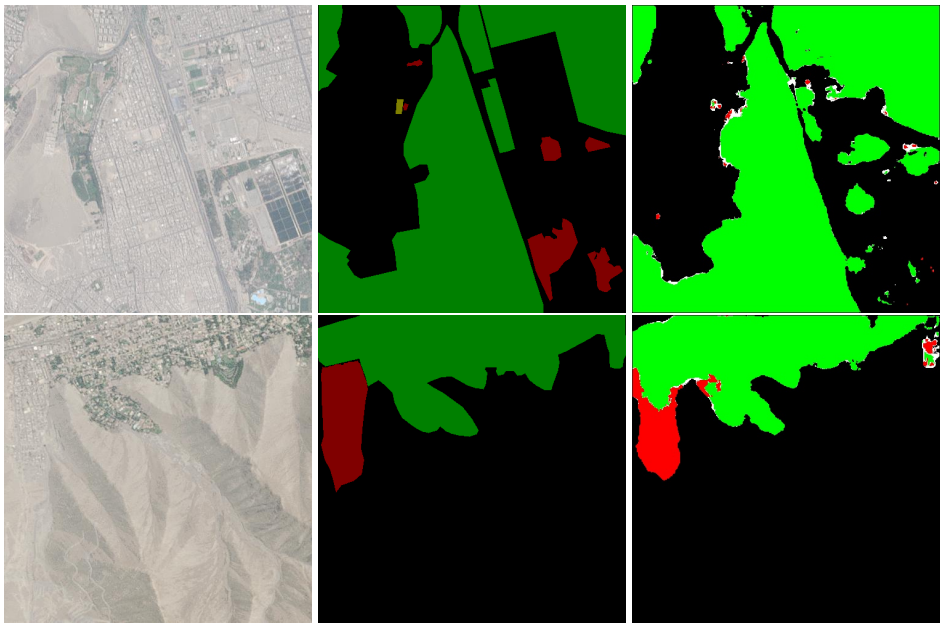

Figure 8: Samples of the results from Task 2. First column has the original images, second column has the ground truth mask an the third has the predicted mask.

## E APPENDIX: FLOOD SUSCEPTIBILITY MAP

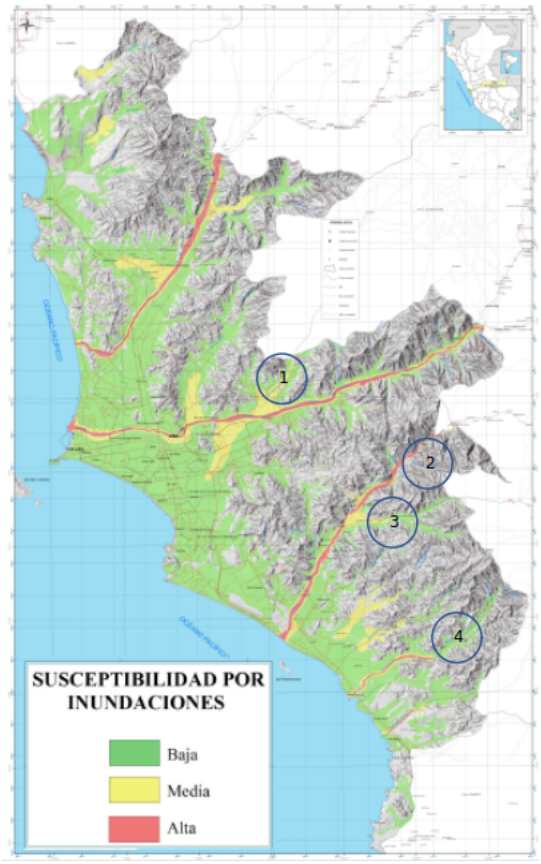


Figure 9: The flood susceptibility map provided by INGMMET. The blue circles indicate areas found by the algorithm with a high potential risk. Image from Villacorta Chambi et al. Peligros geológicos en el área de Lima Metropolitana y la región Callao N°59(Lima:Instituto Geológico, Minero y Metalúrgico,2015)